Supporting Information

Microwave-Assisted Synthesis of Nanoamorphous ($Ni_{0.8}$,$Fe_{0.2}$) Oxide Oxygen Evolving Electrocatalyst Containing Only "Fast" Sites

Joseph M. Barforoush, Dylan T. Jantz, Tess E. Seuferling, Kelly R. Song, Laura C. Cummings and Kevin C. Leonard*

Center for Environmentally Beneficial Catalysis, Department of Chemical and Petroleum Engineering, The University of Kansas, Lawrence, KS, USA, 66047

* Corresponding Author e-mail: kcleonard@ku.edu

1.0 SUPPORTING MATERIALS AND METHODS

1.1 Electrode Fabrication

1.1.1 Drop-cast Thin Films:

FTO glass sheets (Sigma Aldrich) cut to 0.5-inch squares were cleaned by washing with soap, deionized water, and ethanol. The FTO pieces were placed in a beaker with ethanol and sonicated for 10 minutes. The slides were dried at room temperature for about 5 minutes. Then, using a micropipette, approximately 250 μL of solution was dropped onto each square in the most even thin layer possible. The slides were then placed into an oven at 135°C for about 30 minutes. This was repeated once more for a second coating. After coating the FTO glass, the crystalline thin-film samples were fired in air at 500 °C for 3 hours with a 1°C min^{-1} ramp rate. For each sample, a 2-3 mm edge of coating was scraped off and copper wire tape (Electron Microscopy Sciences) was placed on and scored.

1.1.2 Drop-cast solution-derived and microwave-assisted films:

FTO glass sheets were cut and cleaned as described above. Using a micropipette, approximately 250 μL of the suspension was dropped onto each square in the most even thin layer possible. The slides were then placed into an oven at 70°C for about 30 minutes. This was repeated once more for a second coating. No additional annealing was applied to the electrode. For suspensions where separation occurred, the suspension was pipetted from the bottom of the container.

1.1.3 Masked Substrate:

The substrate in the scanning electrochemical microscopy (SECM) experiment was a catalyst sample drop-cast on FTO glass (Sigma-Aldrich) and masked to create a pseudo-ultramicroelectrode suitable for surface interrogation mode of SECM. To make the mask, a 2 cm x 2 cm square of Teflon FEP Film (50A, American Durafilm) was taped to a Teflon block, which was fixed in the clamp of a CNC Mill. A hole was drilled in the FEP film with a 100 μm diameter drill bit (One Piece, Drill Bits Unlimited). The FEP film mask was placed over the catalyst-coated FTO glass with the hole centered and the excess FEP film trimmed off. The masked substrate was placed in the furnace above 271 °C for 30 minutes to allow the FEP film to heat-bond to the substrate.

1.1.4 Glassy Carbon Ultramicroelectrode:

The glassy carbon (GC) ultramicroelectrode utilized as the SECM tip was fabricated similar to the procedure previously reported with some modifications.[15] A 1 cm GC rod (type 2, 1 mm diameter, Alfa Aesar) was electrochemically etched in 4 M KOH by submersing half of the rod and applying 5 V using a graphite counter electrode for 500 s. Subsequently, the rod was flipped and the other end of the rod was electrochemically etched in the same manner. The etching process was repeated, alternating the end of the rod and lowering the etch time as needed, until a sharp GC needle was obtained. The GC needle was rinsed with acetone and deionized water and allowed to dry completely. A silver connection wire (30 AWG, Belden, USA) coated with conductive silver epoxy (Circuit Works, USA) was inserted into one end of a borosilicate glass capillary (1 mm O.D., 0.5 mm I.D., Sutter Instruments, USA). The other end of the borosilicate glass capillary was filled with silver epoxy and the etched GC needle with one end coated in silver epoxy was inserted. The conductive wire was pushed against the GC needle inside the capillary to ensure good electrical contact. The silver epoxy in the electrode was dried in the oven at 120 °C for 30 minutes with the

GC tip pointing upwards. The GC tip was completely coated in epoxy (1C&EPKC, Loctite Hysol) and dried in the oven with the GC tip pointing upwards at 120 °C, removing the electrode to recoat/remold the epoxy every 20 s until sufficiently coated. Finally, the electrode was dried in the oven at 120 °C for 2 hours to hasten the curing of the epoxy. After the epoxy was fully cured, the tip of the electrode was polished with MicroCloth polishing disks (Beuhler, Canada) until a GC disc was visible. The electrode tip was also sharpened with the MicroCloth polishing disc until the desired RG was reached. Before experimentation, the GC disc was polished with alumina micropolish (1 μm, Beuhler, Canada) until it possessed a mirror-like surface.

1.2 Synthesis

1.2.1 Redox Mediator:

The Fe(III)-TEA solution was prepared according to a previously reported procedure.[1] Briefly, 3.2 g of NaOH were added to 10 mL of deionized water while stirring and cooling in a 25 °C water bath. Separately, 20 mL of deionized water was bubbled with argon in a round-bottom flask for 5 minutes. While stirring, 214.4 mg of $Fe_2(SO_4)_3$•xH2O were added to the round-bottom flask. 104 μL of triethanolamine (TEA) were added dropwise to the round-bottom flask. The NaOH solution was added dropwise to the Fe(III) + ligand solution and the volume was adjusted to 40 mL with deionized water.

1.2.2 Crystalline IrO_x:

The crystalline thin-films of IrO_x were made similar to the crystalline-derived $Ni_{0.8}$:$Fe_{0.2}$ described in the main paper. Briefly, a solution of 0.02 M $IrCl_3$ was prepared in ethylene glycol, and the solution was drop-cast and annealed on FTO coated glass (further details can be found in Electrode Fabrication section).

2.0 SUPPORTING FIGURES

Table S1. Performance comparisons between the results of this study and other recent studies on (Ni,Fe) electrocatalysts for the oxygen evolution reaction.

	$\eta_{t=0}$ [mV] (10 mA cm^{-2})	$\eta_{t=2h}$ [mV] (10 mA cm^{-2})	η_{CV}[mV] (10 mA cm^{-2})	η_{CV} [mV] (100 mA cm^{-2})	j_g, [mA cm^{-2}] (η=0.35 V)	j_s, [mA cm-2] (η=0.35 V)	Roughness Factor
This Study	**286**	**315**	**250**	**369**	**61.5**	**55.2**	**1.4**
IrO_x[2]	320 ± 40	1050 ± 20	-	-	42 ± 13	0.4 ± 0.2	105
$NiFeO_x$[2]	350 ± 10	380 ± 20	-	-	15 ± 6	3 ± 2	6
LDH $Ni_{0.9}Fe_{0.1}O_x$[3]	-	-	336	-	-	-	-
Electrodeposited NiFe (40% Fe)[4]	280	-	-	-	-	20 (at 0.3 V)	2-6
LDH NiFe on Graphene Oxide[5]	-	-	221	-	-	-	-
Fractal NiFe[6]	-	-	-	300	-	-	-
Amorphous Ni-Fe oxyhydroxide[7]	300	-	-	-	-	-	-
Pulse-Electrodeposited Ni–Fe (Oxy)hydroxide[8]	-	-	250	-	-	-	-
Laser Ablation $Ni_{0.22}Fe_{0.78}$ LDH[9]	280	-	-	-	-	-	-

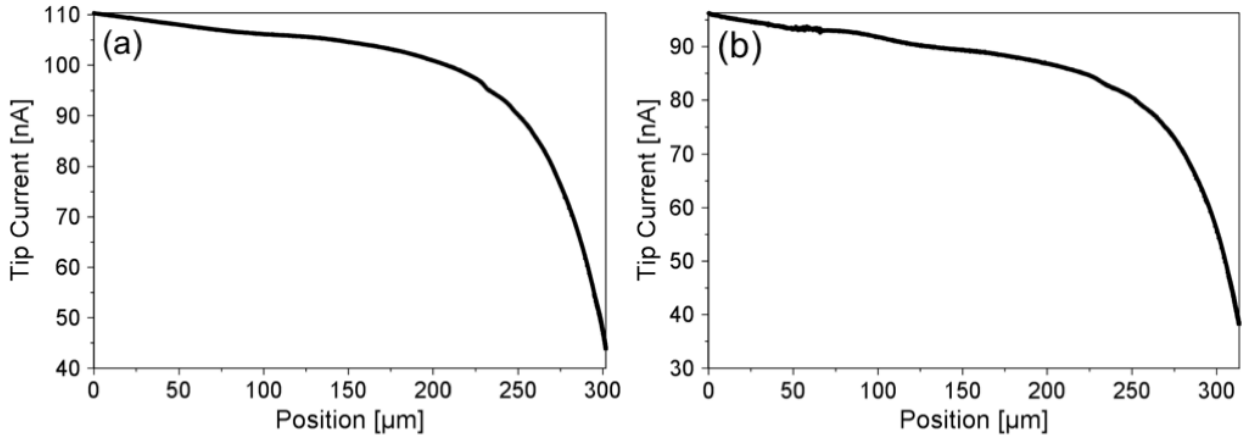

Figure S1. Examples of negative feedback approach curves for imaging and surface interrogation scanning electrochemical microscopy (SI-SECM). Negative feedback approach curve for SI-SECM experiments with glassy carbon ultramicroelectrode tip and masked crystal-derived $Ni_{0.8}$:$Fe_{0.2}$ (a) and microwave-assisted $Ni_{0.8}$:$Fe_{0.2}$ (b) on FTO glass substrate.

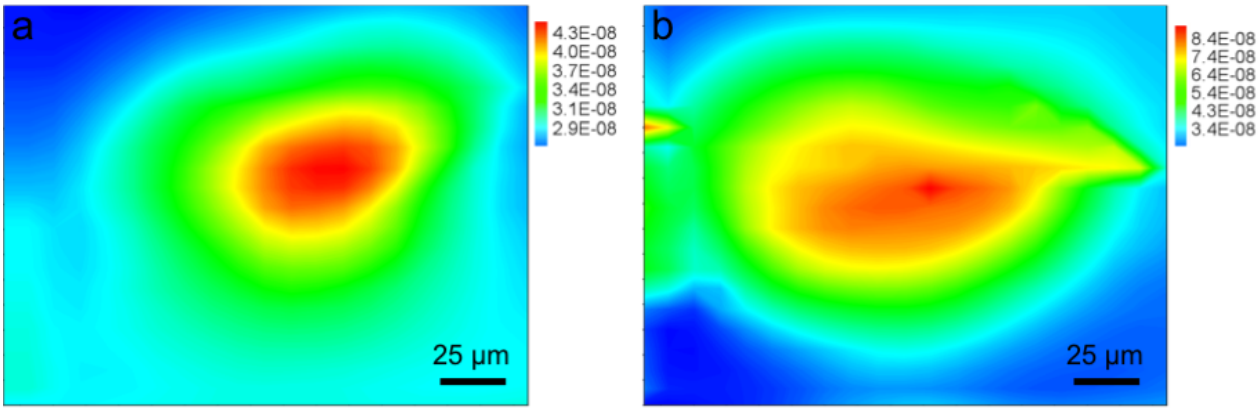

Figure S2. Electrochemical imaging maps for surface interrogation scanning electrochemical microscopy. Map of the hole in the mask on crystal-derived $Ni_{0.8}$:$Fe_{0.2}$ (a) and microwave-assisted $Ni_{0.8}$:$Fe_{0.2}$ (b) on FTO glass substrate generated using a glassy carbon ultramicroelectrode tip with Fe(III)/Fe(II)-TEA redox couple. High reduction current is represented as red, revealing the location of the mask hole, and low reduction current is shown as blue.

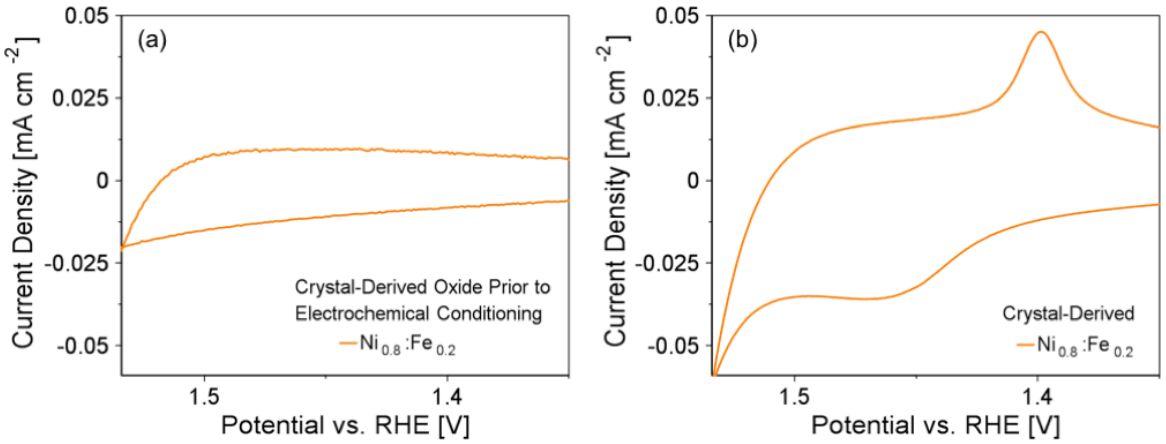

Figure S3. Cyclic voltammograms (CVs) of the crystal-derived $Ni_{0.8}$:$Fe_{0.2}$ before (a) and after (b) applying an electrochemical conditioning oxidation current of c.a. 10 mA for 1 h to create an oxyhydroxide morphology with characteristic peaks appearing in the CVs between 1.45 and 1.5 V vs RHE. The CV after electrochemical conditioning is a magnified view of the crystal-derived CV presented in Figure 3a of the main text.

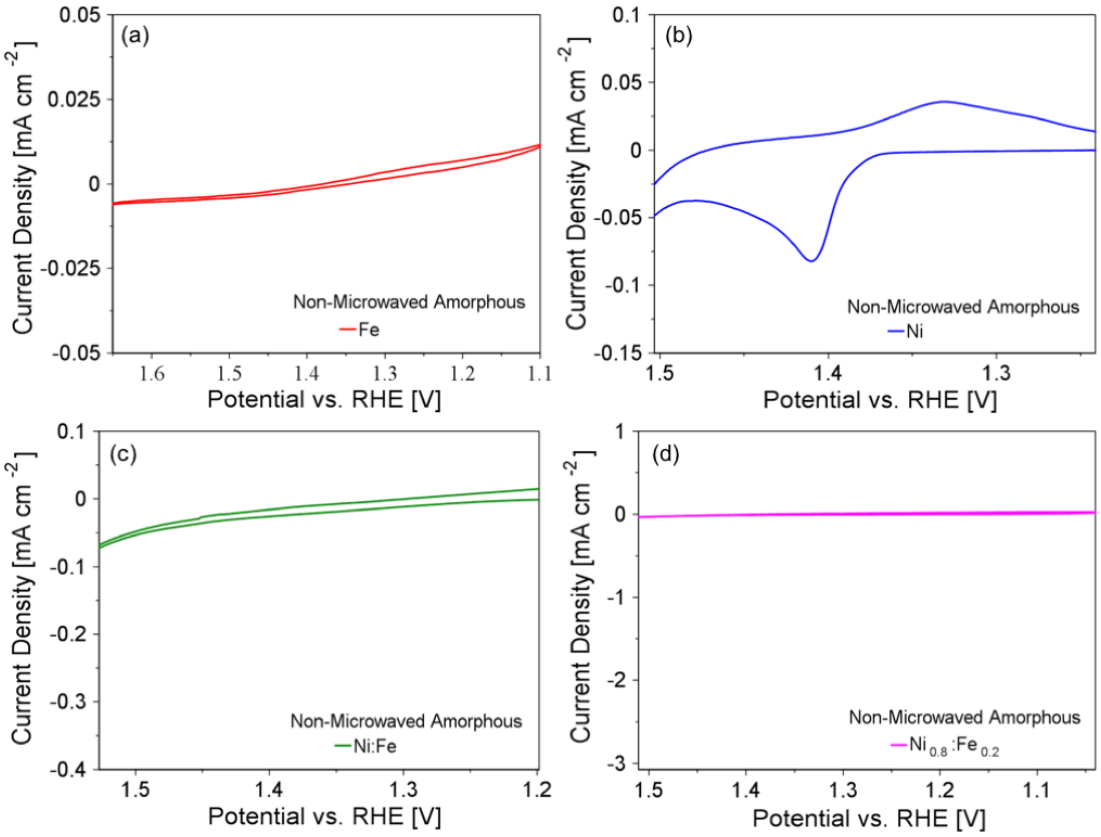

Figure S4. Cyclic voltammograms (CVs) of the solution-derived Fe (a), Ni (b), Ni:Fe (c), and $Ni_{0.8}$:$Fe_{0.2}$ (d) on FTO-coated glass. Each CV was taken from Figure 1a of the main text and magnified to the region where the Ni^{II}/Ni^{III} peaks would be visible. The Ni is the only one of our solution-derived materials to show the characteristic oxyhydroxide peaks before microwaving.

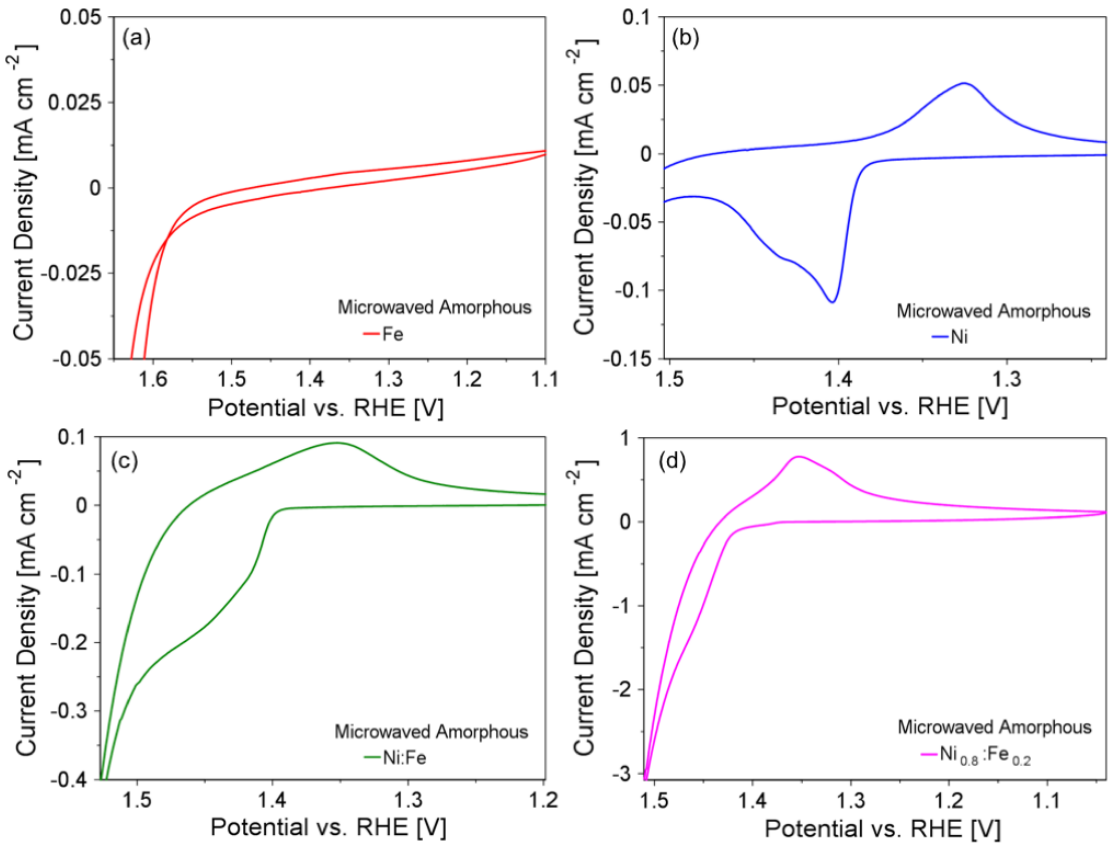

Figure S5. Cyclic voltammograms (CVs) of the microwave-assisted Fe (a), Ni (b), Ni:Fe (c), and $Ni_{0.8}$:$Fe_{0.2}$ (d). Each CV was taken from Figure 1a of the main text and magnified to the region where the Ni^{II}/Ni^{III} peaks are visible. As expected, the Fe is the only one of our microwave-assisted materials to lack the characteristic peaks.

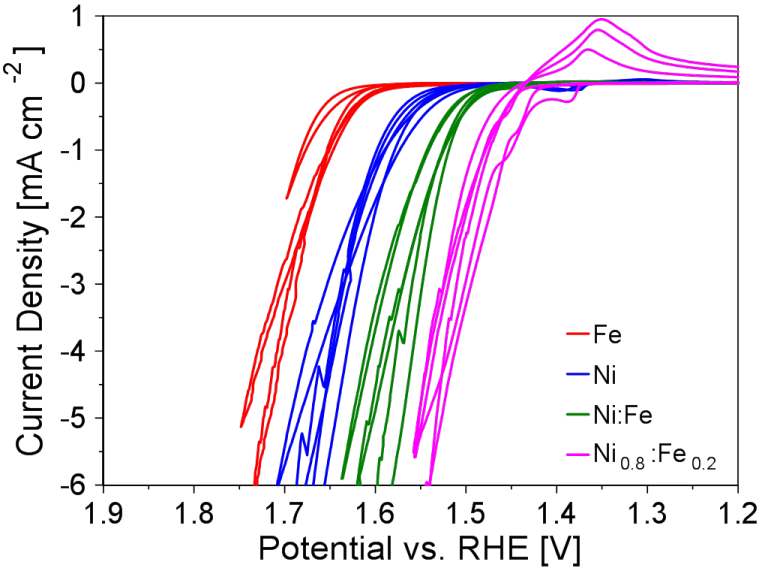

Figure S6. Experimental cyclic voltammograms (CVs) in 1 M NaOH at a scan rate of 1 mV s^{-1} not corrected for R_u for three different batches of microwave-assisted Fe, Ni, Ni:Fe, and $Ni_{0.8}$:$Fe_{0.2}$ coated on FTO glass using the convention of reduction currents as positive and negative potentials to the right. Each CV shown is from a freshly fabricated microwave-assisted metal/mixed metal (oxy)hydroxide.

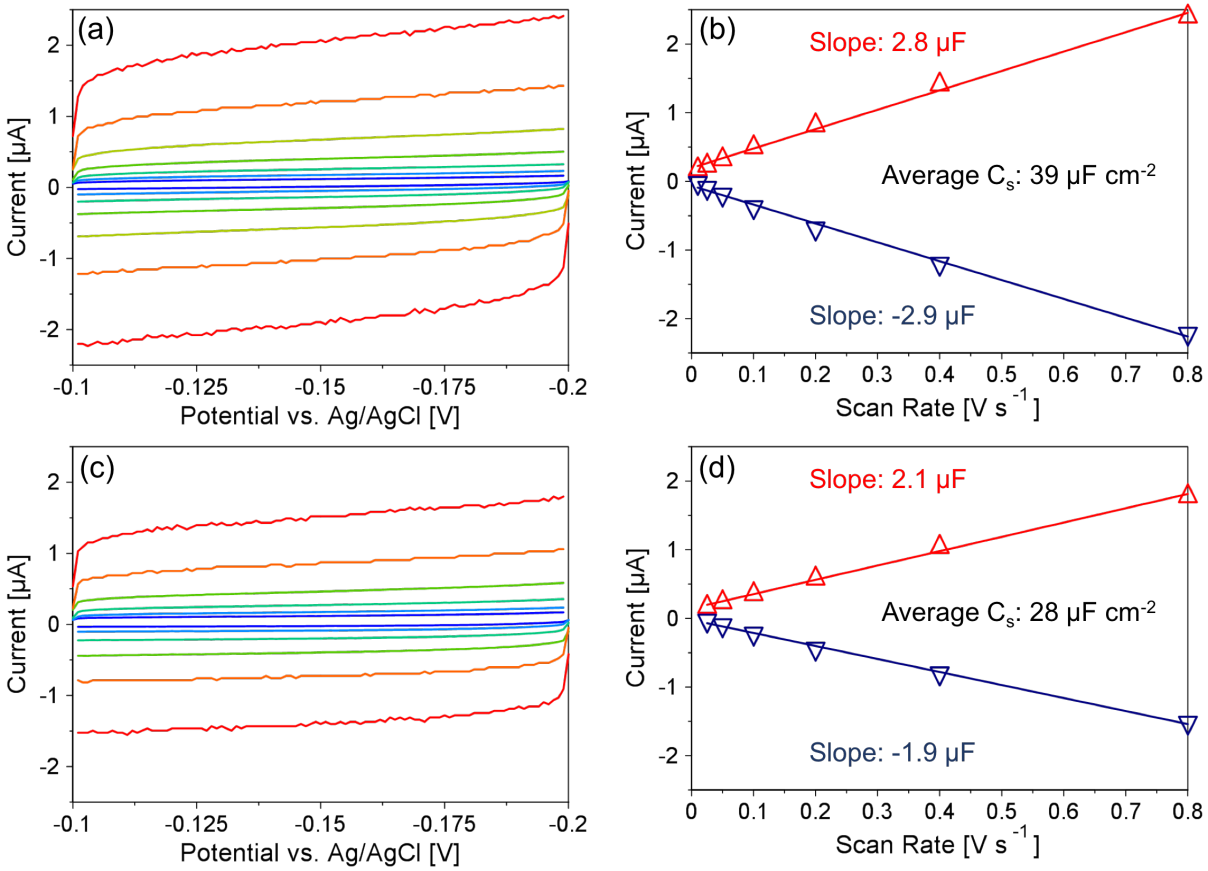

Figure S7. Double-layer capacitance measurements via cyclic voltammetry on microwave-assisted $Ni_{0.8}$:$Fe_{0.2}$ electrodeposited on glassy carbon (a) and bare glassy carbon (c) in 1M NaOH at various scan rates where non-faradaic current occurs. Current vs scan rate for microwave-assisted $Ni_{0.8}$:$Fe_{0.2}$ electrodeposited on glassy carbon (b) and bare glassy carbon (d) with regression lines next to the corresponding double layer capacitance values and the average specific capacitance, C_s.

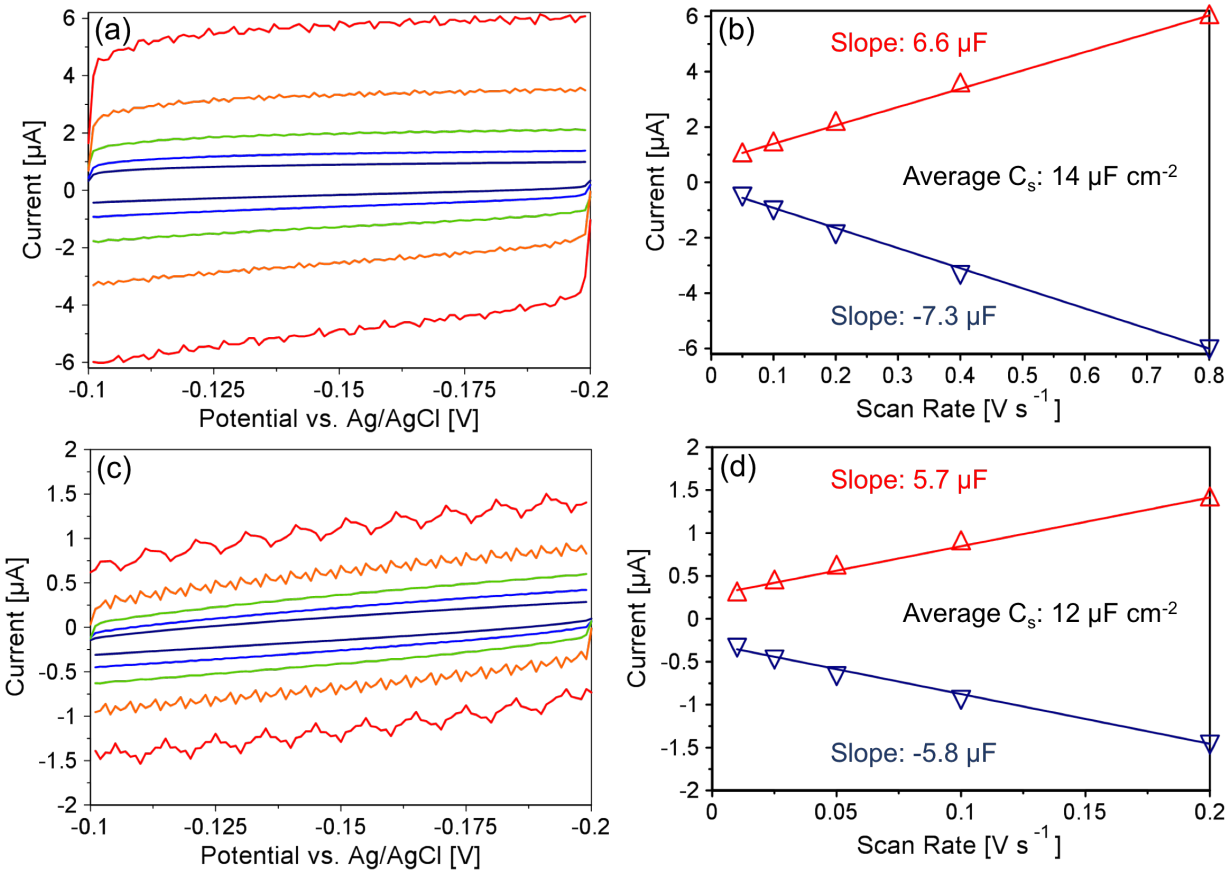

Figure S8. Double-layer capacitance measurements via cyclic voltammetry on crystal-derived $Ni_{0.8}$:$Fe_{0.2}$ oxyhydroxide on FTO-coated glass (a) and bare FTO-coated glass (c) in 1M NaOH at various scan rates where non-faradaic current occurs. Current vs scan rate for crystal-derived $Ni_{0.8}$:$Fe_{0.2}$ oxyhydroxide on FTO-coated glass (b) and bare FTO-coated glass (d) with regression lines next to the corresponding double layer capacitance values and the average specific capacitance, C_s.

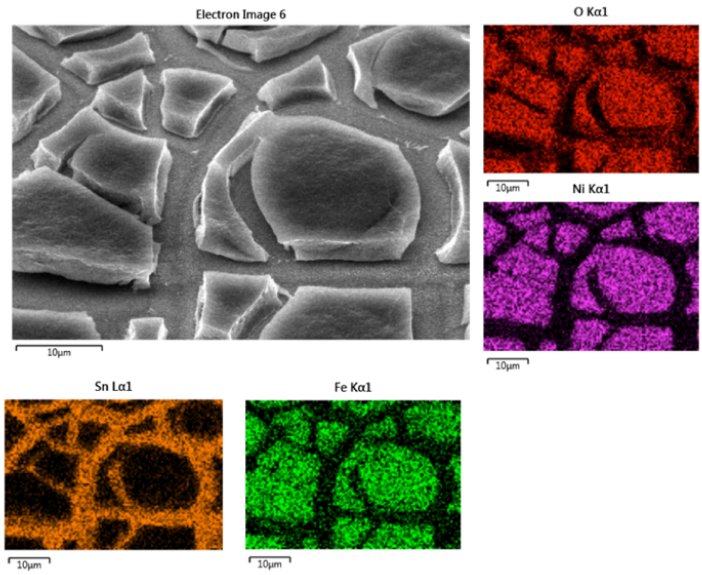

Figure S9. SEM and corresponding EDS images of crystal-derived $Ni_{0.8}$:$Fe_{0.2}$ sample prior to electrochemical conditioning step. Shown is the uniform distribution of Fe and Ni along with the Sn of the sub-layer due to the FTO coated glass substrate.

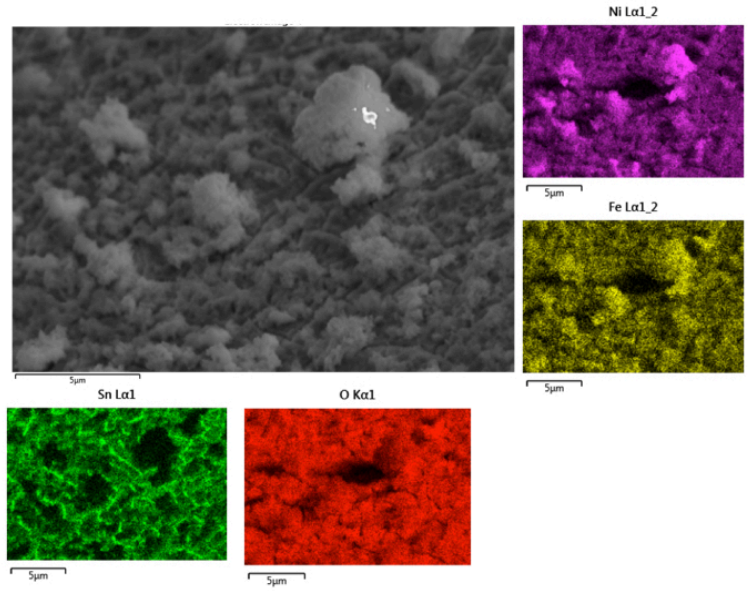

Figure S10. SEM and corresponding EDS images of microwave-assisted, nanoamorphous $Ni_{0.8}$:$Fe_{0.2}$ sample electrophoretically deposited on a FTO coated glass substrate. Shown is the uniform distribution of Fe and Ni along with the Sn of the sub-layer due to the FTO coated glass substrate.

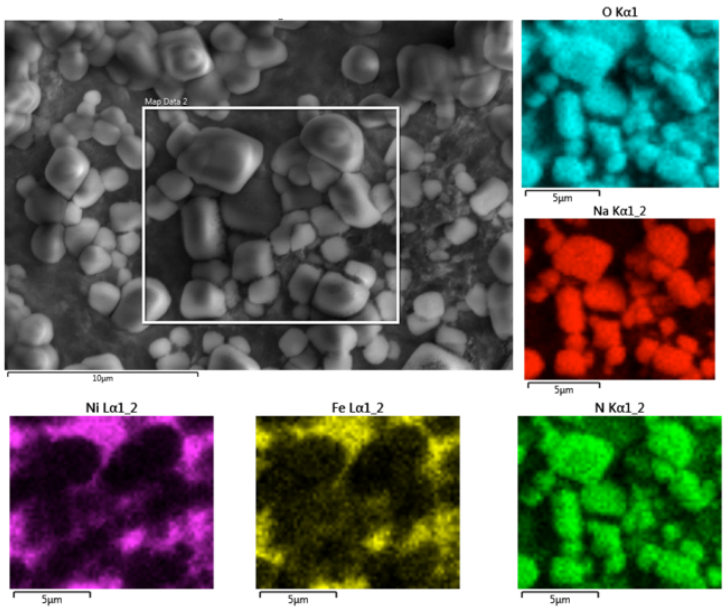

Figure S11. SEM and corresponding EDS images of the microwave-assisted $Ni_{0.8}$:$Fe_{0.2}$ sample without the rinsing step. Shown are the $NaNO_3$ crystal that are a result of titration of $NaHCO_3$ with Fe or Ni NO_3. These $NaNO_3$ crystals are also present in the XRD patterns of the microwave-assisted samples.

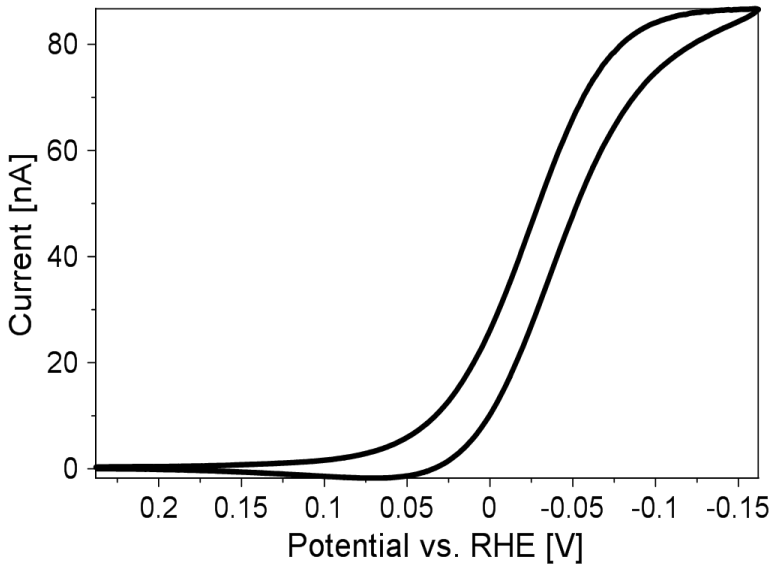

Figure S12. Redox mediator, c.a. 50 mM Fe(III)-TEA, cyclic voltammogram (CV) at 10 mV s^{-1} in 2 M NaOH with a glassy carbon ultramicroelectrode.

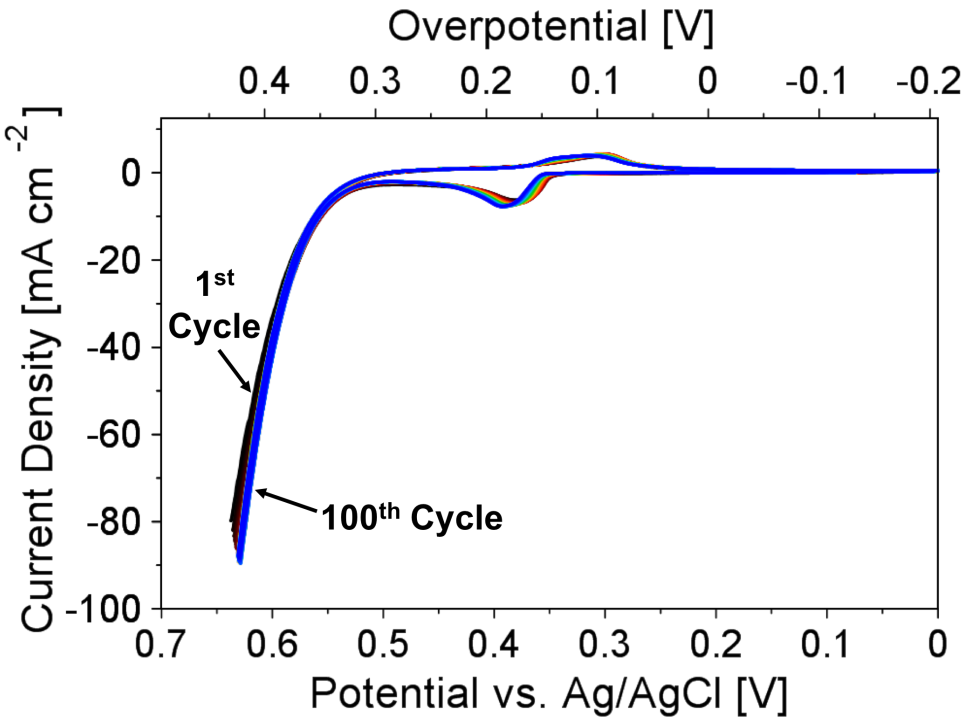

Figure S13. 100 cyclic voltammetry (CV) cycles at 50 mV s^{-1} on microwave-assisted nanoamorphous $Ni_{0.8}$:$Fe_{0.2}$ electrodeposited on a glassy carbon electrode in 1 M NaOH and corrected for R_u showing no significant change in activity with each successive cycle.

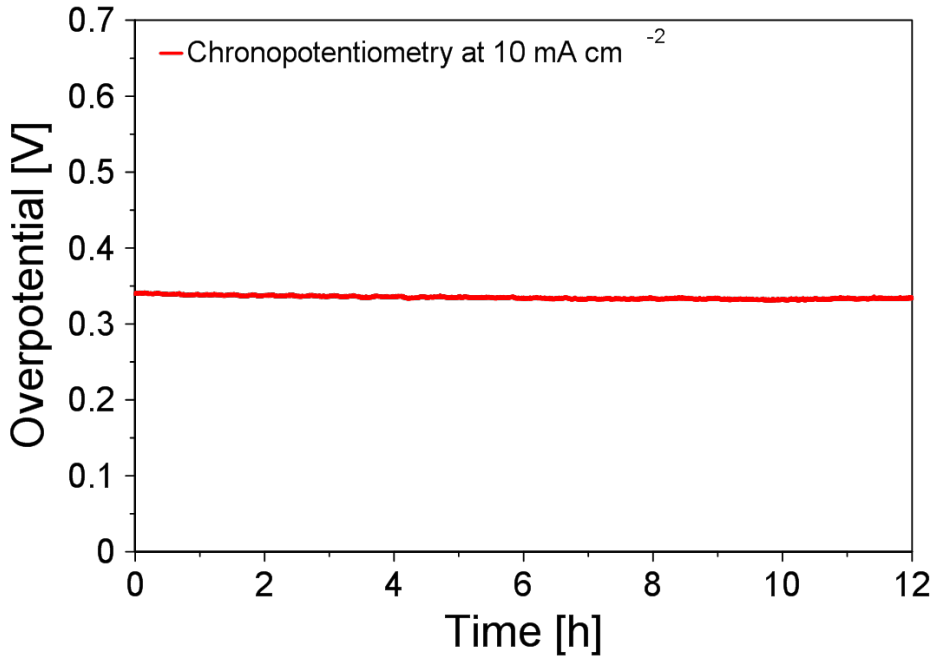

Figure S14. 12 h chronopotentiometry experiment at 10 mA cm^{-2} with microwave-assisted nanoamorphous $Ni_{0.8}$:$Fe_{0.2}$ electrodeposited on a glassy carbon RDE at 1600 rpm in 1 M NaOH and corrected for R_u showing stable oxygen production with an overpotential of 0.33 V at 12 h.

3.0 DETAILS ON COMSOL MULTIPHYSICS SIMULATIONS:

COMSOL (COMSOL Multiphysics v. 5.2) simulations were performed to obtain the negative feedback current for the SI-SECM experiments. In COMSOL a 2D axial-symmetric domain was created to simulate the actual size of our SECM tip electrode, the size and thickness of the masked catalyst electrode, and the tip/substrate distance as described in the main paper (Figure S14). Two separate edge meshes were used, (1) on the SECM tip boundary, and (2) on the catalyst electrode boundary extending up and halfway across the FEP mask. These edge meshes had a maximum element size of 0.5 μm and a minimum element size of 0.05 μm. A free triangular mesh was used for the solution using COMSOL's built-in "fine" element size, which was calibrated for fluid dynamics. Figure S13 shows 2D axial-symmetric geometry with the mesh used for these simulations.

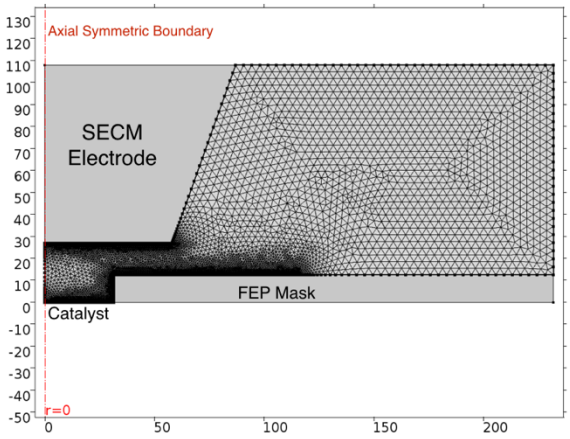

Figure S15. COMSOL 2D axial-symmetric domain and corresponding mesh used for SI-SECM simulations.

The COMSOL Electroanalysis module was used to simulate the SECM tip current during the surface interrogation experiment. This module couples Fick's Law of Diffusion with the Butler-Volmer Equation to obtain the concentration of the oxidized and reduced species in solution, as well as the current on the electro-active boundary as a function of applied potential. Since the reduction of Fe(III)-TEA to Fe(II)-TEA is a fast outer-sphere, one-electron transfer, we used 1 cm/s as the electron-transfer kinetic rate constant and α = 0.5 for the transfer coefficient. The diffusion coefficient for both the Fe(III)-TEA and Fe(II)-TEA species was 2E-6 cm^2/s as previously reported.[1] The tip potential in our simulations was exactly as it was in our experiment. The tip/substrate distance was 7 microns above the surface of the FEP mask. The initial concentration of redox mediator, Fe(III)-TEA, used was 28 mM for the crystal-derived $Ni_{0.8}$:$Fe_{0.2}$ and 65 mM for the microwave-assisted $Ni_{0.8}$:$Fe_{0.2}$ (different concentrations of redox mediator were attributed to evaporative losses of solution from argon bubbling in between experiments).

4.0 SUPPORTING REFERENCES:

1. N. Arroyo-Currás and A. J. Bard, *J. Phys. Chem. C*, 2015, **119**, 8147-8154.
2. C. C. McCrory, S. Jung, J. C. Peters and T. F. Jaramillo, *J. Am. Chem. Soc.*, 2013, **135**, 16977-16987.
3. L. Trotochaud, J. K. Ranney, K. N. Williams and S. W. Boettcher, *J. Am. Chem. Soc.*, 2012, **134**, 17253-17261.
4. M. W. Louie and A. T. Bell, *J. Am. Chem. Soc.*, 2013, **135**, 12329-12337.
5. X. Long, J. Li, S. Xiao, K. Yan, Z. Wang, H. Chen and S. Yang, *Angew. Chem.*, 2014, **126**, 7714-7718.
6. T. T. Hoang and A. A. Gewirth, *ACS Catal.*, 2016, **6**, 1159-1164.
7. M. Görlin, M. Gliech, J. F. de Araújo, S. Dresp, A. Bergmann and P. Strasser, *Catal. Today*, 2016, **262**, 65-73.
8. A. S. Batchellor and S. W. Boettcher, *ACS Catal.*, 2015, **5**, 6680-6689.
9. B. M. Hunter, J. D. Blakemore, M. Deimund, H. B. Gray, J. R. Winkler and A. M. Müller, *J. Am. Chem. Soc.*, 2014, **136**, 13118-13121.